Science Advances
AAAS

advances.sciencemag.org/cgi/content/full/6/41/eabb8508/DC1

Supplementary Materials for

Spatial and temporal variations in global soil respiration and their relationships with climate and land cover

Ni Huang, Li Wang*, Xiao-Peng Song, T. Andrew Black, Rachhpal S. Jassal, Ranga B. Myneni, Chaoyang Wu, Lei Wang, Wanjuan Song, Dabin Ji, Shanshan Yu, Zheng Niu

*Corresponding author. Email: wangli@radi.ac.cn

Published 7 October 2020, *Sci. Adv.* **6**, eabb8508 (2020)
DOI: 10.1126/sciadv.abb8508

This PDF file includes:

Supplementary Materials

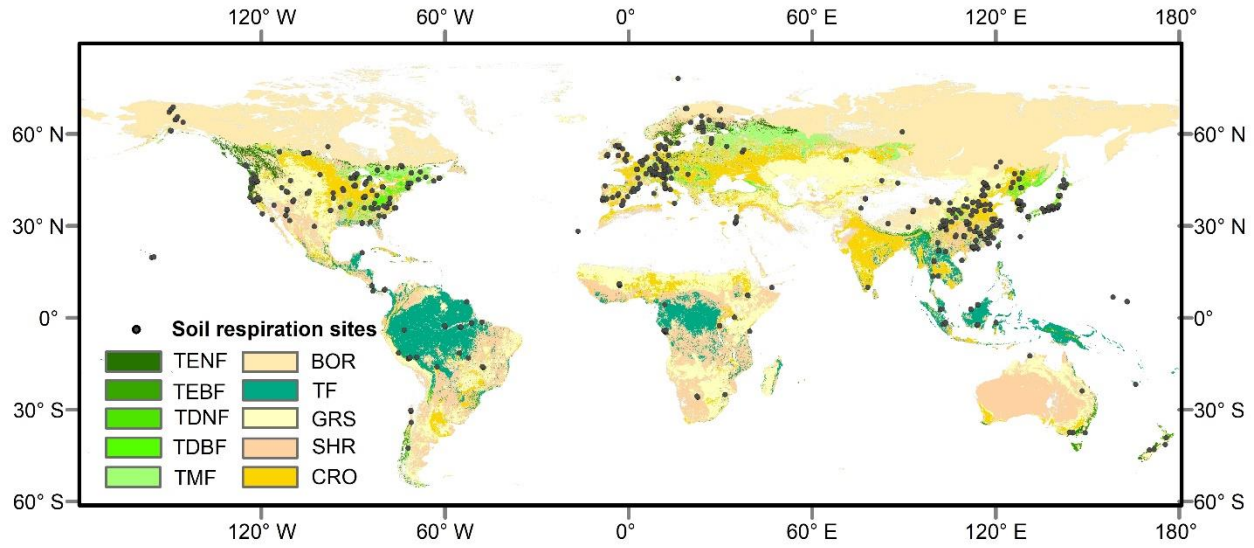

Fig. S1. The spatial distribution of in situ soil respiration (R_s) measurements at the global scale from 2000 to 2014. TENF, temperate evergreen needleleaf forest; TEBF, temperate evergreen broadleaf forest; TDNF, temperate deciduous needleleaf forest; TDBF, temperate deciduous broadleaf forest; TMF, temperate mixed forest; BOR, boreal vegetation; TF, tropical forest; GRS, grasslands; CRO, croplands; SHR, shrublands.

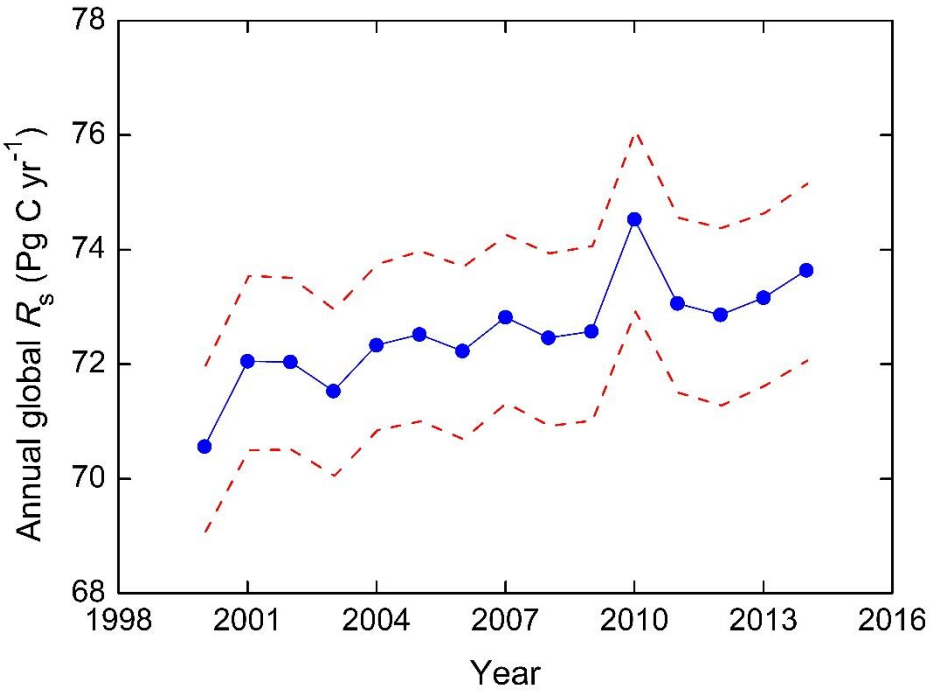

Fig. S2. Estimated annual global soil respiration (R_s) over the period 2000-2014. The two red dashed lines indicate the 95% confidence intervals.

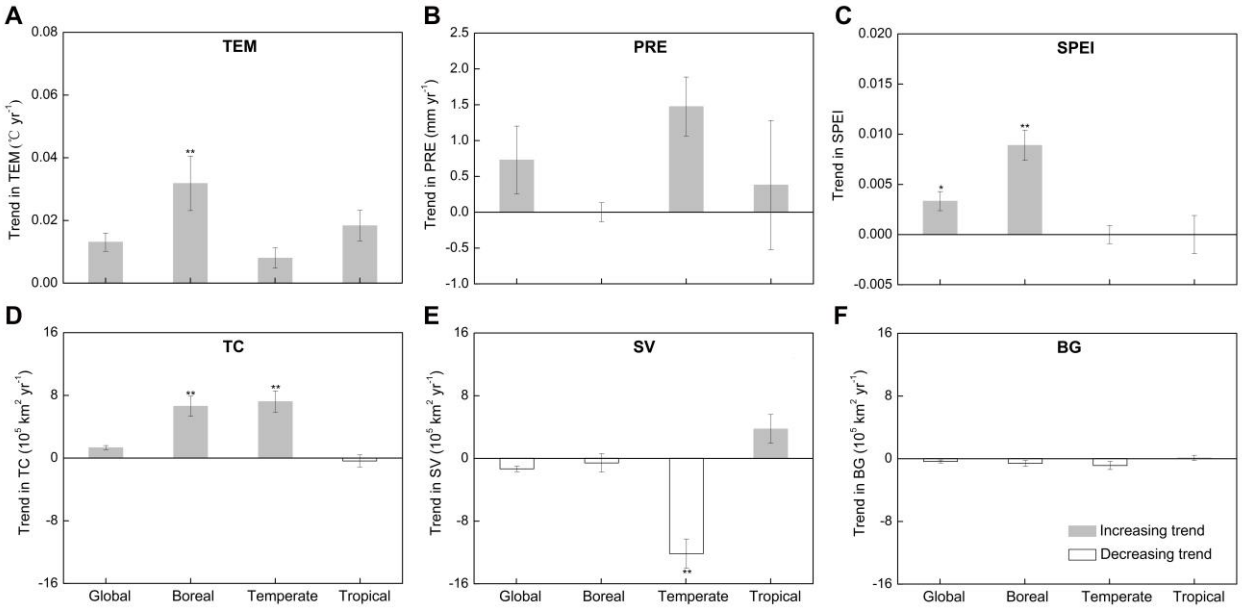

Fig. S3 Trends in climate and land cover factors at global and regional scales from 2000 to 2014. (**A**) Annual mean air temperature (TEM). (**B**) Annual precipitation (PRE). (**C**) Annual mean standardized precipitation–evapotranspiration index (SPEI). (**D**) Tree canopy (TC) cover. (**E**) Short vegetation (SV) cover. (**F**) Bare ground (BG) cover. We denote significant trends ($p<0.05$) with two asterisks and marginally significant trends ($p<0.1$) with one asterisk based on the results of two-sided Mann–Kendall tests. Grey bars in the upward direction indicate an increasing trend during the period, whereas hollow bars in the downward direction indicate a decreasing trend. The error bars indicate the 95% confidence intervals, which were estimated via a 1000 bootstrap analysis.

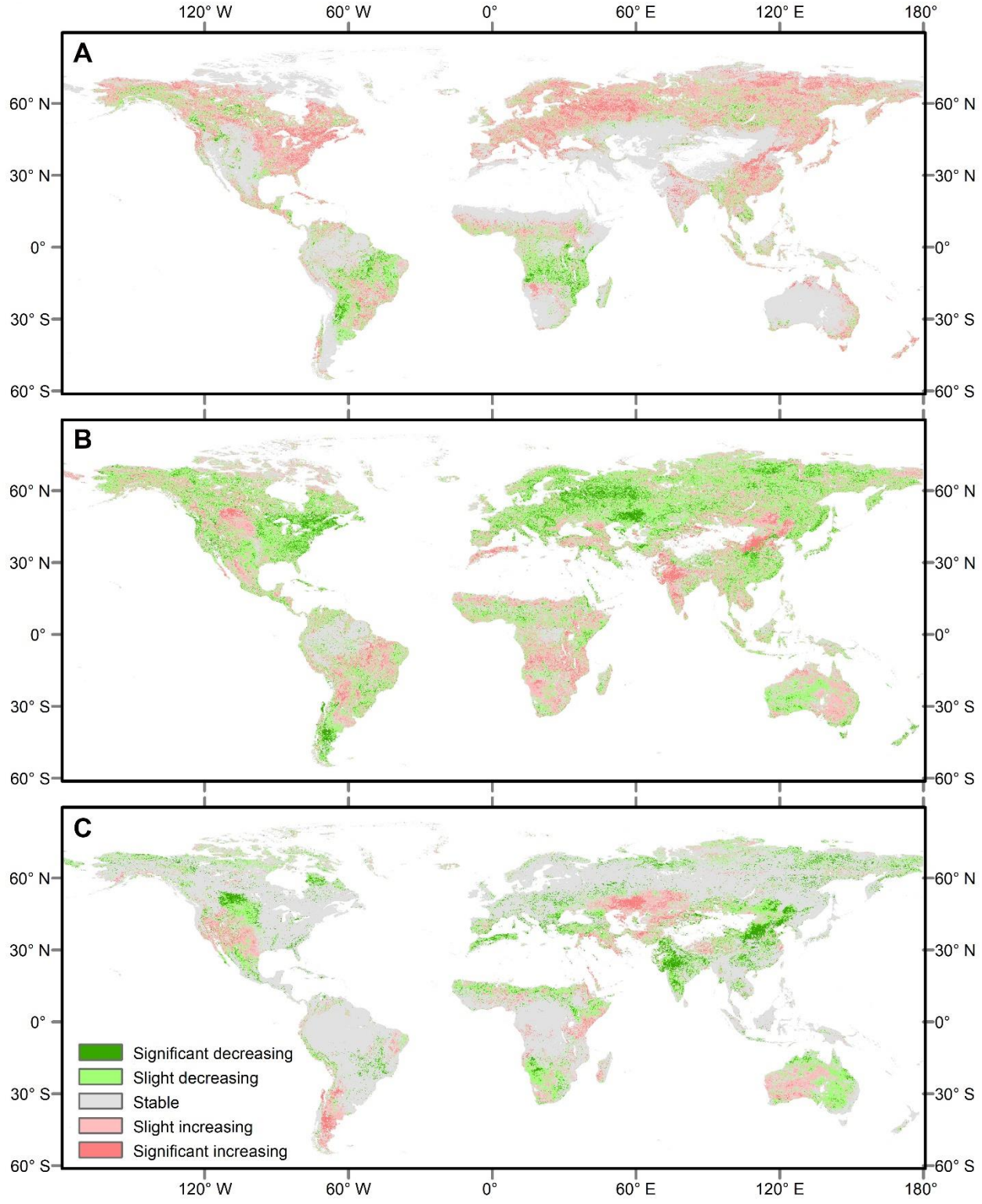

Fig. S4. Global distribution of trends in land covers from 2000 to 2014. (**A**) Tree canopy cover. (**B**) Short vegetation cover. (**C**) Bare ground cover. Significant increasing and decreasing trends correspond to positive and negative Theil-Sen estimators, respectively, with significant Mann-Kendall test ($p<0.05$). Slightly increasing and decreasing trends correspond to positive and negative

Theil-Sen estimators, respectively, with non-significant Mann-Kendall test results ($p>0.05$). The residual pixels belong to a stable class.

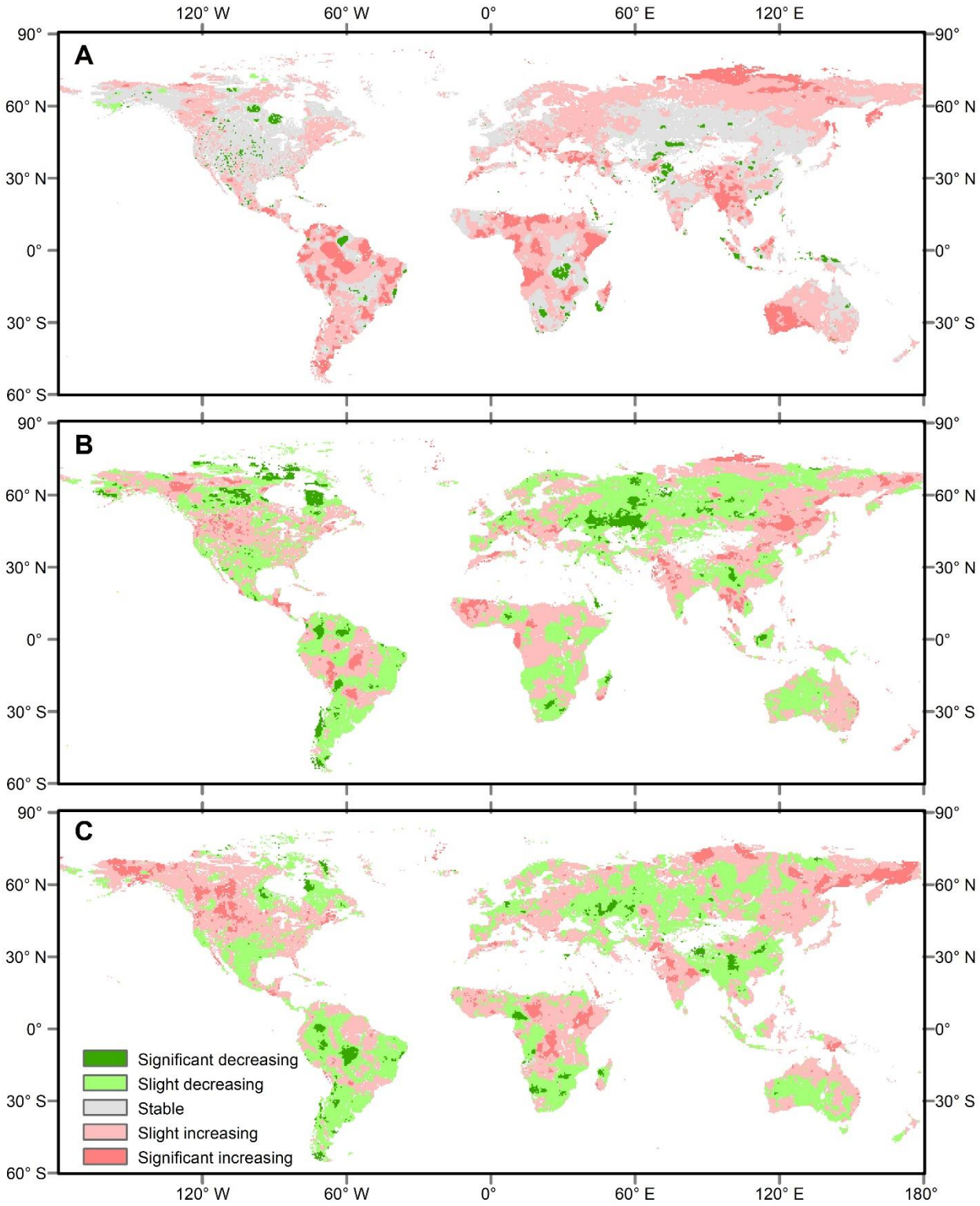

Fig. S5. Global distribution of trends in climate factors from 2000 to 2014. (**A**) Annual mean

air temperature. (**B**) Annual precipitation. (**C**) Standardized precipitation–evapotranspiration index. Significant increasing and decreasing trends correspond to positive and negative Theil-Sen estimators, respectively, with significant Mann-Kendall test ($p<0.05$). Slightly increasing and decreasing trends correspond to positive and negative Theil-Sen estimators, respectively, with non-significant Mann-Kendall test results ($p>0.05$). The residual pixels belong to a stable class.

Table S1. Comparison of global annual soil respiration (R_s) estimates by different studies during a defined period.*

Period	Annual R_s (Pg C yr^{-1})	Increasing rate (Pg C yr^{-1})	Uncertainty/Range (Pg C yr^{-1})	R^2	RMSE (g C m^{-2} yr^{-1})	Spatial resolution	Input data	Reference
1980-1994	80.4		79.3-81.8 (interannual)	0.62	-	0.5 °×0.5 °	Climate data	(*10*)
2008	98	0.1 (1989-2008)	±12 (estimation error at a 95% confidence level)	0.320-0.426	-	0.5 °×0.5 °	Climate data, leaf area index, nitrogen deposition, biome type	(*11*)
1970-2008	94.4	0.04 (1970-2008), not significant (1989-2008)	±8.7 (standard error (SE) of global R_s for 1970), ±9.2 (SE for 2008)	0.47-0.89	150-350	0.5 °×0.5 °	Climate data, soil organic carbon	(*12*)
1980-2009	78	-	64-95 (estimation error at a 95% confidence level)	-	323.2	0.5 °×0.5 °	Climate data	(*13*)
2001-2009	94.8 (2001), 93.8 (2009)	-		-	-	4 km×4 km	MODIS climate data and land-use maps	(*14*)
1961-2011	87.9	-	18.6 (mean absolute error), 40.4 (root mean square error)	0.63	305.2	1 km×1 km	Mean annual temperature, mean annual precipitation, mean annual MODIS enhanced vegetation index, mean precipitation from November through January	(*2*)
1960-2012	93.3	0.04 (1960-2012)	±6.1 (estimation error at a 95% confidence level)	0.6	298	5′×5′	Climate data, biome type	(*15*)
1965-2012	91	0.09 (1965-2012), 0.14 (1990-2012)	88-95 (interannual), 87-95 (estimation error at a 95% confidence level)	0.32	376.8	0.5 °×0.5 °	Climate data	(*9*)

2000-2012	94.3	-	±17.9 (estimation error at a 95% confidence level), 91.3-96.8 (interannual)	-	-	-	Annual R_s, vegetation type data	(*7*)
2014	80.3-108.6	-	24.6-69.6 (propagating the site error and multiplying by the area of the cells)	0.1-0.55	141.97-573.01	0.5 °×0.5 °	Mean soil temperature, mean soil moisture, total soil carbon, MODIS net primary production	(*16*)
1961-2014	78.76	-	±7 (estimation error at a 95% confidence level)	0.87	-	0.5 °×0.5 °	Vegetation classification, climate region classification, elevation data, above-ground biomass, soil organic carbon, climate data	(*17*)
1980-2016	90.8-102.1	-	-	-	-	-	Global average annual soil heterotrophic respiration (RH), global ratio of RH/total soil respiration (0.56-0.63)	(*3*)
2000-2014	72.6	0.13 (2000-2014)	±2.8 (estimation error at a 95% confidence level), 70.6-74.5 (interannual)	0.62-0.84	107-413	1 km×1 km	Remotely sensed temperature, moisture and plant productivity factors	This study

*R^2 is coefficient of determination and RMSE is root mean square error, which describe fit between measured annual R_s and model-estimated annual R_s values. The horizontal line shows that the data is not available.

Table S2. Annual soil respiration (R_s) estimates for different biomes using the 10-fold cross validation technique with four models.*

Biome	n	p	MNLR		RFR		SVR		ANN		Selected model
			R^2	RMSE (g C m^{-2} yr^{-1})	R^2	RMSE (g C m^{-2} yr^{-1})	R^2	RMSE (g C m^{-2} yr^{-1})	R^2	RMSE (g C m^{-2} yr^{-1})	
TENF	264	<0.0001	0.3	308	0.44	267	0.42	272	0.35	302	RFR
TEBF	52	<0.0001	0.52	293	0.68	295	0.58	303	0.56	315	RFR
TDNF	107	<0.0001	0.47	238	0.47	267	0.53	236	0.54	233	SVR
TDBF	206	<0.0001	0.2	274	0.53	221	0.45	226	0.44	227	RFR
TMF	63	<0.0001	0.35	186	0.56	164	0.61	137	0.5	179	SVR
BOR	44	<0.0001	0.5	140	0.65	148	0.69	132	0.53	158	SVR
TF	166	<0.0001	0.36	519	0.57	429	0.46	438	0.54	446	RFR
GRS	182	<0.0001	0.48	392	0.64	269	0.57	280	0.62	279	RFR
CRO	66	<0.0001	0.55	254	0.58	312	0.51	341	0.48	351	RFR
SHR	64	<0.0001	0.45	251	0.58	242	0.58	239	0.56	259	SVR

* Biome labels are as described in fig. S1. Four models are multiple nonlinear regression (MNLR), random forest regression (RFR), support vector regression (SVR), and artificial neural network (ANN).

Table S3. Selected model and predictive variables for each biome for estimation of annual soil respiration (R_s).*

Biome	Selected model	Selected predictive variables			n	p	R^2	RMSE (g C m^{-2} yr^{-1})
		Temperature	Moisture	Plant productivity				
TENF	RFR	LST_night_spring	LST_diff_annual	GPP_summer	264	<0.0001	0.71	209
TEBF	RFR	LST_night_summer	LST_diff_annual	GPP_annual	52	<0.0001	0.65	269
TDNF	SVR	LST_night_spring	LST_diff_spring	GPP_spring	107	<0.0001	0.74	191
TDBF	RFR	LST_night_summer	LST_diff_annual	GPP_annual	206	<0.0001	0.62	202
TMF	SVR	LST_night_annual	ET_spring	GPP_annual	63	<0.0001	0.81	119
BOR	SVR	LST_day_annual	ET_summer	NDVI_annual	44	<0.0001	0.74	107
TF	RFR	LST_night_spring	LST_diff_annual	NDVI_annual	166	<0.0001	0.63	413
GRS	RFR	LST_night_annual	LST_diff_annual	NDVI_annual	182	<0.0001	0.63	264
CRO	RFR	LST_night_annual	ET_PET_spring	NDVI_annual	66	<0.0001	0.77	267
SHR	SVR	LST_day_summer	LST_diff_summer	NDVI_annual	64	<0.0001	0.84	153

*The selected model is based on the model ranking of the 10-fold cross-validation. The calculation of the fitting accuracy (i.e., p, R^2, and root mean square error (RMSE)) is based on the within-sample statistics. Biome labels are as described in fig. S1. RFR is random forest regression and SVR is support vector regression. Selected predictive variables are described in Materials and Methods subsection “Available predictive variables for annual soil respiration estimation”.

Table S4. Parameters of the selected models for soil respiration (R_s) estimation for each biome.*

Biome	Selected model	Parameters	Parameter interpretation
TENF	RFR	NumTrees =400, predictor-splitting algorithm="standard CART", NumPredictorsToSample="all"	Standard CART means "Selects the split predictor that maximizes the split-criterion gain over all possible splits of all predictors".
TEBF	RFR	NumTrees =400, predictor-splitting algorithm="Interaction test", NumPredictorsToSample="all"	
TDNF	SVR	Epsilon=32.1720, Standardize="false", Solver="SMO", KernelScale=1, KernelFunction=" gaussian"	SMO means "Sequential Minimal Optimization"
TDBF	RFR	NumTrees =800, predictor-splitting algorithm="standard CART", NumPredictorsToSample="all"	Standard CART means "Selects the split predictor that maximizes the split-criterion gain over all possible splits of all predictors".
TMF	SVR	Epsilon=18.7824, Standardize="false", Solver="SMO", KernelScale=1, KernelFunction="gaussian"	SMO means "Sequential Minimal Optimization"
BOR	SVR	Epsilon=26.9088, Standardize="True", Solver="SMO", KernelScale=2.1733, KernelFunction="gaussian"	
TF	RFR	NumTrees =800, predictor-splitting algorithm="Interaction test", NumPredictorsToSample="all"	
GRS	RFR	NumTrees =300, predictor-splitting algorithm="standard CART", NumPredictorsToSample="all"	Standard CART means "Selects the split predictor that maximizes the split-criterion gain over all possible splits of all predictors".
CRO	RFR	NumTrees =400, predictor-splitting algorithm="Interaction test", NumPredictorsToSample="all"	
SHR	SVR	Epsilon=36.8236, Standardize="false", Solver="SMO", KernelScale=1, KernelFunction="gaussian"	SMO means "Sequential Minimal Optimization"

*Biome labels are as described in fig. S1. RFR is random forest regression and SVR is support vector regression.

Table S5. Partial correlation coefficient among tree canopy (TC) cover, short vegetation (SV) cover and bare ground (BG) cover at different latitudinal bands from 2000 to 2014.*

Latitudinal bands	Partial correlation coefficient		
	TC and SV	TC and BG	SV and BG
> 55 °N	-1.00	-0.99	-0.99
35–55 °N	-1.00	-0.99	-0.99
15–35 °N	-0.98	-0.96	-0.99
15 °N to 15 °S	-1.00	-1.00	-1.00
15–35 °S	-0.99	-0.98	-1.00
35–55 °S	-1.00	-1.00	-1.00

*The partial correlation coefficient was calculated by conducting partial correlation analyses between spatially averaged annual soil respiration and six controlling factors (annual mean air temperature, annual precipitation, standardized precipitation–evapotranspiration index, TC cover, SV cover, BG cover) from 2000 to 2014 at six different latitudinal bands. The partial correlations among the three land-cover factors were all statistically significant at $p<0.0001$.

Supplementary material for methods

1. Variable importance analysis for the machine learning algorithm models

The variable importance was analyzed by using a removal-based approach to avoid the limited interpretability of the machine learning algorithms (RFR, SVR, and ANN). All the algorithms were adjusted N times, with N being the number of available

variables. At each time, one variable was removed to quantify the RMSE of the algorithm, and then all the RMSEs were normalized by the largest RMSE. A normalized RMSE represents the relative importance of variance and varies between 0 and 1. The variable with the highest relative importance contributed most to the performance of the machine learning algorithm models.

2. Descriptive statistics of the integrated soil respiration database

At the global scale, annual R_s measurements were obtained for a wide range of biomes (table S6). Among the ten biomes, most of the R_s measurements were obtained from TENF (n=269), followed by TDBF (n=230), and only 53 and 47 from TEBF and BOR, respectively. The annual R_s, mean annual temperature (MAT) and mean annual precipitation (MAP) vary widely within and among the biomes (table S6). In most biomes, the standard deviation (SD) of annual R_s, MAP and MAT exceeded 40% of their mean values. The biome mean annual R_s was highest in the TF, with the mean annual R_s of 1198 g C m^{-2} yr^{-1} and SD of 638 g C m^{-2} yr^{-1}, which corresponded to the highest biome mean MAT (22.7 ℃) and MAP (1993 mm). Such a high R_s in TF was expected as the high temperature and precipitation that support soil metabolic activity also support plant growth and thus R_s. The biome mean annual R_s was intermediate in temperate forest biomes (ranging from 786 g C m^{-2} yr^{-1} to 864 g C m^{-2} yr^{-1}) and lowest in the coldest BOR (450 g C m^{-2} yr^{-1}). Multiple comparisons showed that the mean annual R_s were significantly different between the forest and non-forest biomes, which may be explained by the differences in MAT and MAP (table S6).

Table S6. Summary statistics of mean annual soil respiration (R_s, g C m^{-2} yr^{-1}), mean annual air temperature (MAT, ℃) and mean annual precipitation (MAP, mm) across biomes based on the integrated global R_s database. *

Biome	R_s			MAT			MAP		
	n	Mean (SD)	Range	n	Mean (SD)	Range	n	Mean(SD)	Range
TENF	269	786 (367)[a]	34-2194	190	8.9 (4.4)[a]	-1.4-22.0	218	1222 (596)[a]	265-3502
TEBF	53	864 (422)[a]	201-1813	48	13.5 (3.6)[b]	1.9-23.5	50	1201 (536)[ab]	368-3341
TDNF	114	859 (321)[a]	275-2304	97	8.9 (4.5)[a]	0.7-20.7	101	1056 (364)[b]	240-2122
TDBF	230	840 (306)[a]	38-2548	188	9.6 (4.2)[a]	-1.4-19.9	192	1019 (466)[b]	125-2400
TMF	66	804 (232)[a]	232-1763	63	8.5 (4.0)[a]	1.5-21.3	62	1045 (375)[b]	398-2175
BOR	47	450 (198)[b]	58-721	23	-0.4 (2.5)[c]	-5.4-4.6	24	460 (166)[d]	181-960
TF	178	1198 (638)[c]	71-4140	143	22.7 (3.9)[d]	2.1-34.5	164	1993 (1034)[e]	280-5302
GRS	185	770 (545)[a]	56-3141	161	8.9 (6.9)[a]	-5.6-31	170	739 (494)[f]	102-3000
CRO	84	629 (449)[d]	72-2939	74	12.6 (6.3)[b]	1.6-30.0	76	931 (689)[b]	102-5000
SHR	66	630 (345)[d]	38-1324	56	13.5 (6.9)[b]	-1.4-29.5	53	656 (399)[df]	90-1900

* Biome labels are as described in fig. S1. The Mean (and standard deviation (SD)) within a column followed by different letters are significantly different ($p<0.05$).

3. The relationships between annual soil respiration and remotely sensed temperature, moisture or plant productivity variables at global and biome scales

On a global scale, the biome mean annual R_s showed significantly positive relationships ($p<0.01$) with MAT, MAP, and GPP_annual, with R^2 values of 0.64, 0.84, and 0.71, respectively (fig. S6). This result, consistent with previous studies (*7*,*16*), demonstrated that globally annual R_s is positively correlated with MAT, MAP, and mean GPP_annual. These relationships are highly dependent upon the global biome data used. Any difference in R^2 and significance level between our study and the previous studies may be due to the differences in the time period covered and partitioning of the R_s dataset into global biomes (*7*,*16*).

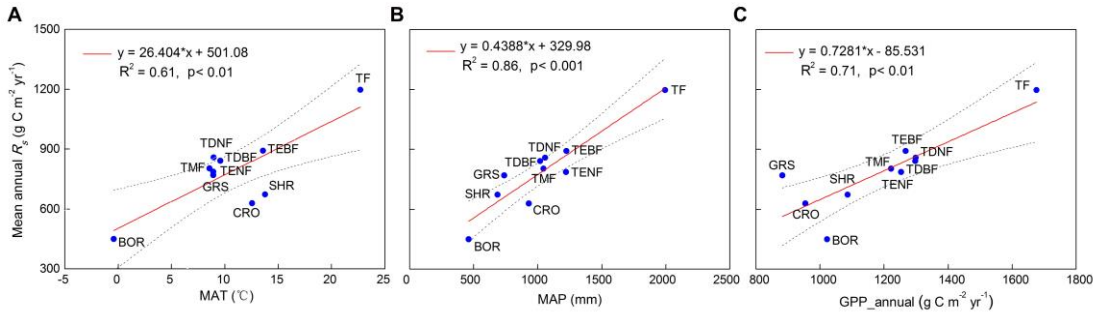

Fig. S6. The linear regression relationships between the biome mean annual soil respiration (R_s, g C m^{-2} yr^{-1}) and abiotic or biotic factors at global scale. (**A**) Mean annual air temperature (MAT, ℃). (**B**) Mean annual precipitation (MAP, mm). (**C**) Mean annual plant gross primary productivity (GPP_annual, g C m^{-2} yr^{-1}). The annual R_s, MAT and MAP data are from the integrated global database. GPP_annual is from MODIS MOD17A2H product. Biome labels are as described in fig. S1.

Based on the pooled data from the integrated global R_s database, MAT and MAP showed a significantly strong positive linear relationship ($p<0.0001$) with remotely

sensed LST_night_annual and RS_pre_annual, respectively (fig. S7), which demonstrated the feasibility of using remote sensing data instead of climate data to estimate global R_s. Further analysis of the relationships between annual R_s and these influencing factors quantified by remote sensing data at the biome scale showed that the significant relationships existing at the global scale changed at the biome scale. The Pearson's correlation coefficient (r) for the relationships between annual R_s and remotely sensed temperature, moisture or plant productivity variables at annual, spring, or summer time scales showed appreciable differences among the ten biomes (figs. S8 to S10). Hursh et al. (*16*) also demonstrated that the relative degree of importance among factors known to regulate R_s at the biome scale were significantly different from those at the global scale.

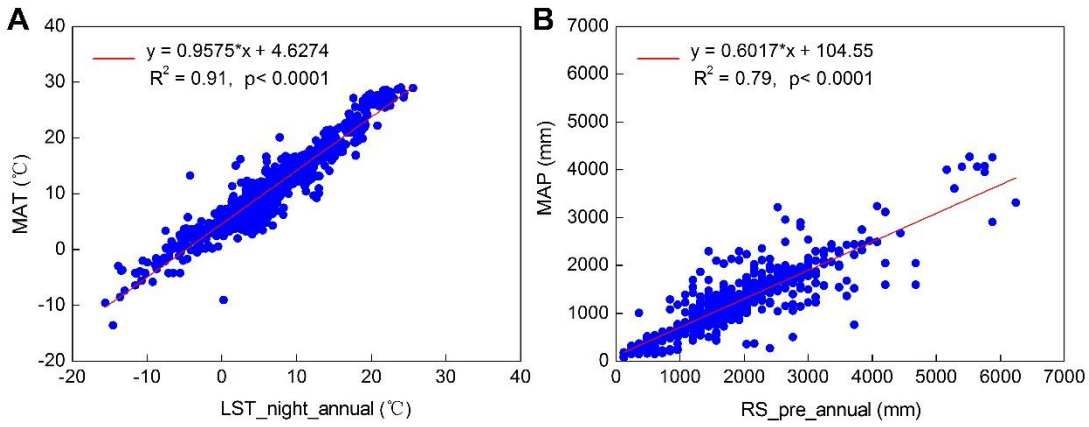

Fig. S7. The linear regression relationships between remotely sensed abiotic factors and their corresponding observed values. (**A**) The relationship between mean annual air temperature (MAT, ℃) and MOD11A2 land surface temperature at nighttime at an annual time scale (LST_night_annual). (**B**) The relationship between

mean annual precipitation (MAP, mm) and remotely sensed precipitation data from TRMM 3B43 at an annual time scale (RS_pre_annual).

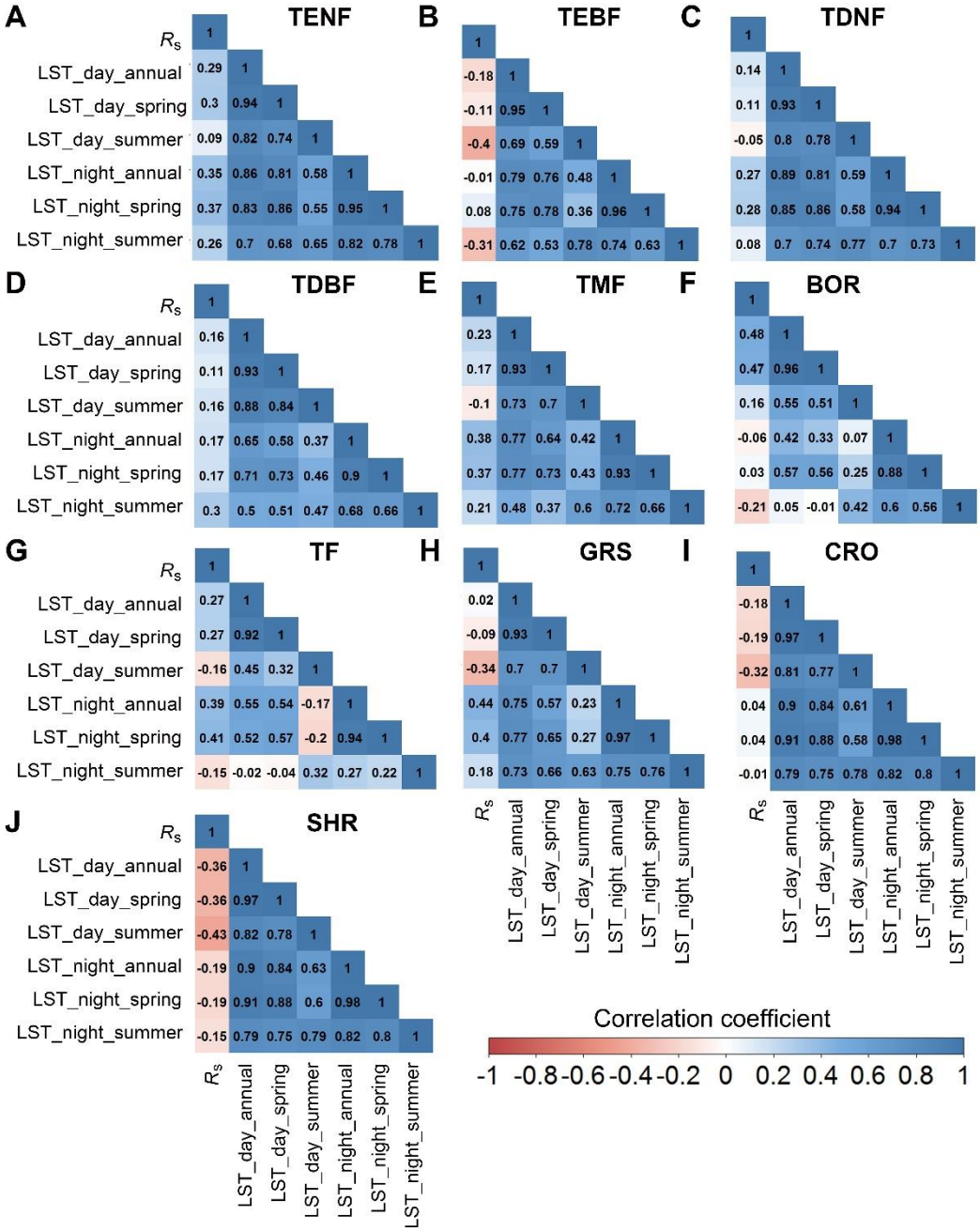

Fig. S8. Pearson's correlation coefficient (r) between the mean annual soil respiration (R_s) and remotely sensed temperature variables. Biome labels are as described in fig. S1.

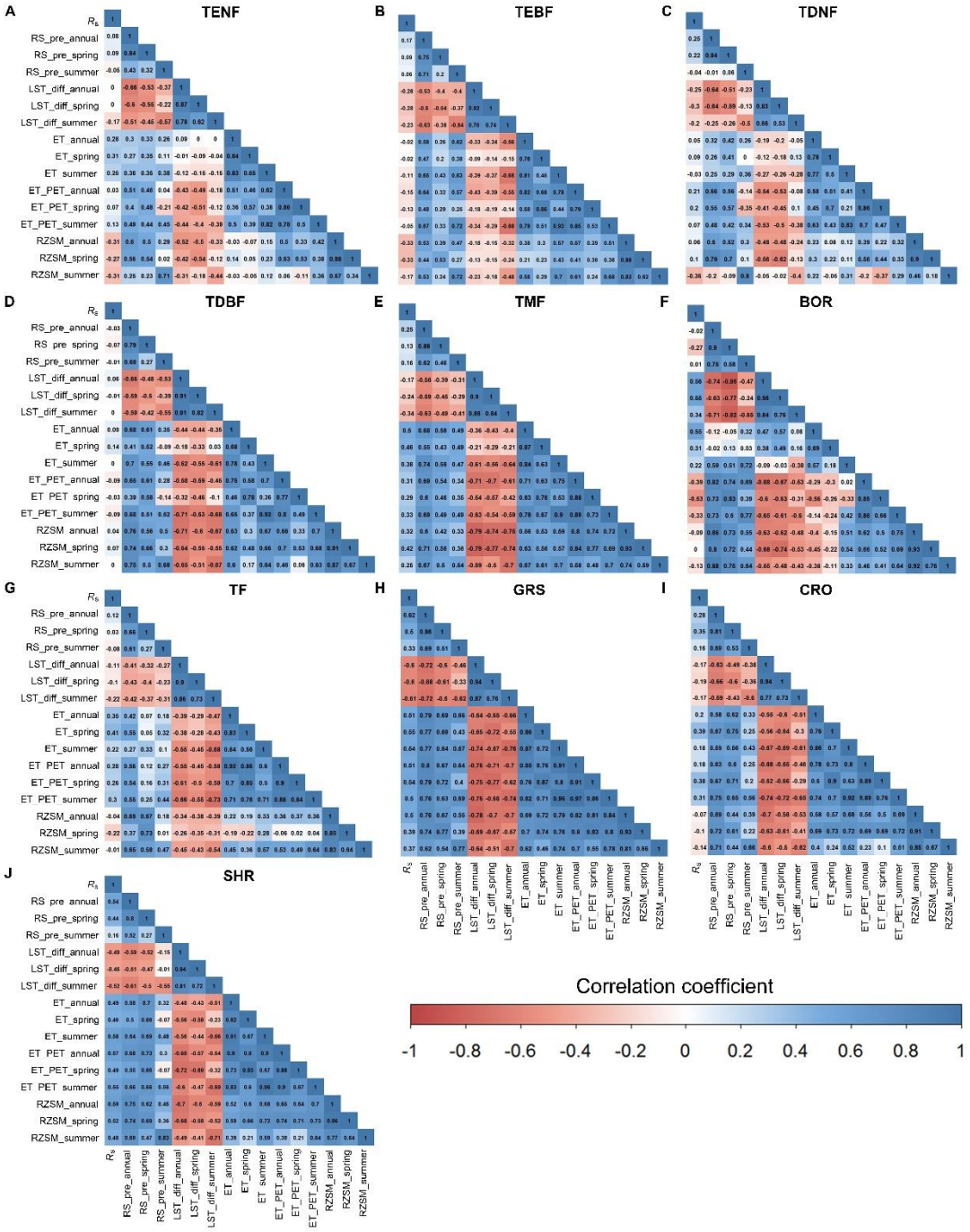

Fig. S9. Pearson's correlation coefficient (r) between the mean annual soil respiration (R_S) and remotely sensed moisture variables. Biome labels are as described in fig. S1.

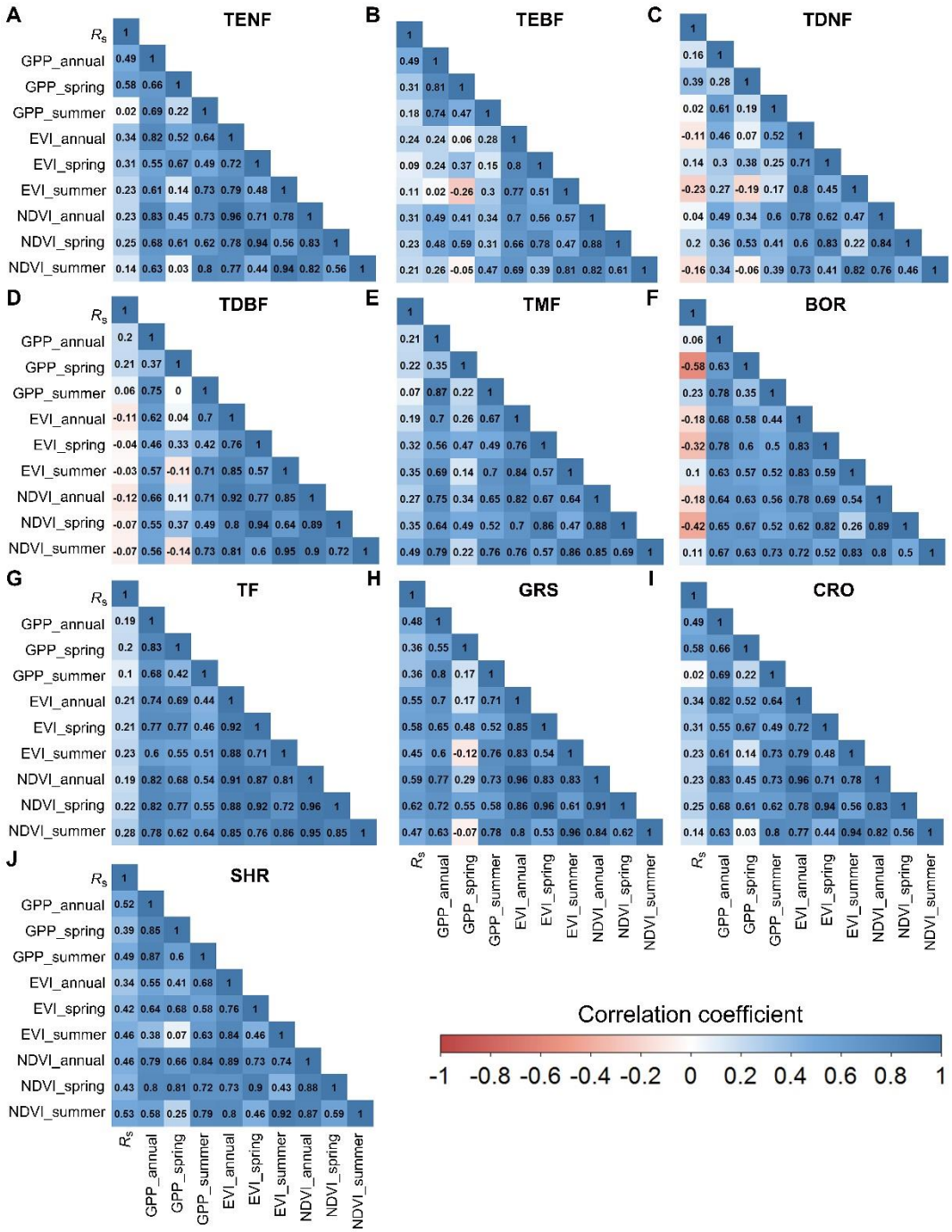

Fig. S10. Pearson's correlation coefficient (r) between the mean annual soil respiration (R_s) and remotely sensed plant productivity variables for each biome. Biome labels are as described in fig. S1.

For all biomes, most of the temperature, moisture or plant productivity variables were highly correlated ($r>0.8$, $p<0.001$, figs. S8 to S10). Furthermore, value of r between the

three types of variables at the annual and spring time scales is higher than that at the summer time scale. The r between annual R_s and the three types of remotely sensed variables (temperature, moisture, and plant productivity) varied with biome types in both direction and magnitude (figs. S8 to S10). In most biomes, the r between annual R_s and the three types of variables (temperature, moisture and plant productivity) at the annual time scale is similar to that at the spring time scale. Not considering the biome type and time scale of variables, at least one variable showed a significantly negative or positive correlation with annual R_s for each biome ($p<0.01$), although the magnitude of r changes with biome types. Almost all the temperature variables at temperature limited biomes (e.g., TENF), and all the moisture variables in water-limited biomes (e.g., GRS and SHR) showed significant correlations with annual R_s ($p<0.01$, figs. S8 and S9). In addition, significant correlations were found between annual R_s and plant productivity variables for TNEF, GRS and SHR ($p<0.01$, fig. S10).

4. The variables selected to estimate annual soil respiration

By selecting the variables corresponding to maximum ρ (figs. S11 to S13), we determined the optimal variables for annual R_s estimation (table S7). Based on ρ values for Eqs. 2-4 (figs. S11 to S13), we found that different input of remotely sensed temperature variables resulted in greater differences in model explanatory power (i.e., $0.25\times\frac{\mathrm{RMSE}_{min}}{\mathrm{RMSE}}$ and $0.25\times\frac{R^2}{R^2_{max}}$) than observation data representation (i.e., $0.5\times\frac{n}{n_{max}}$) within one biome, and the opposite phenomenon was observed for remotely sensed moisture and plant productivity variables. Furthermore, the data source and time

scale of the selected temperature, moisture and plant productivity variables for the annual R_s estimation are not consistent across biomes (table S7). This result was expected because empirical analyses are not universally robust across biomes.

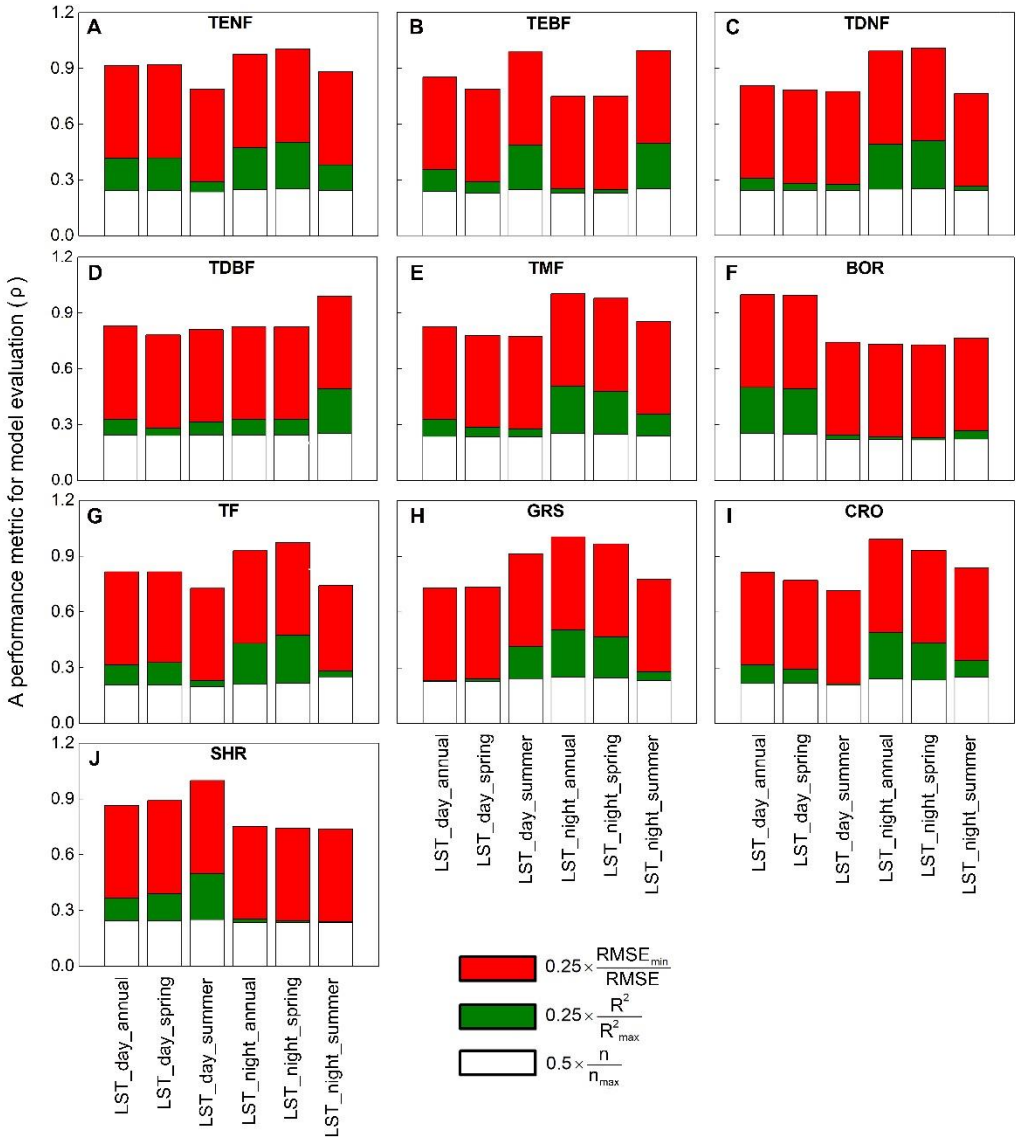

Fig. S11. The performance metric for model evaluation (ρ) for Eq. (2) with different inputs of remotely sensed temperature variables for each biome. Biome labels are as described in fig. S1.

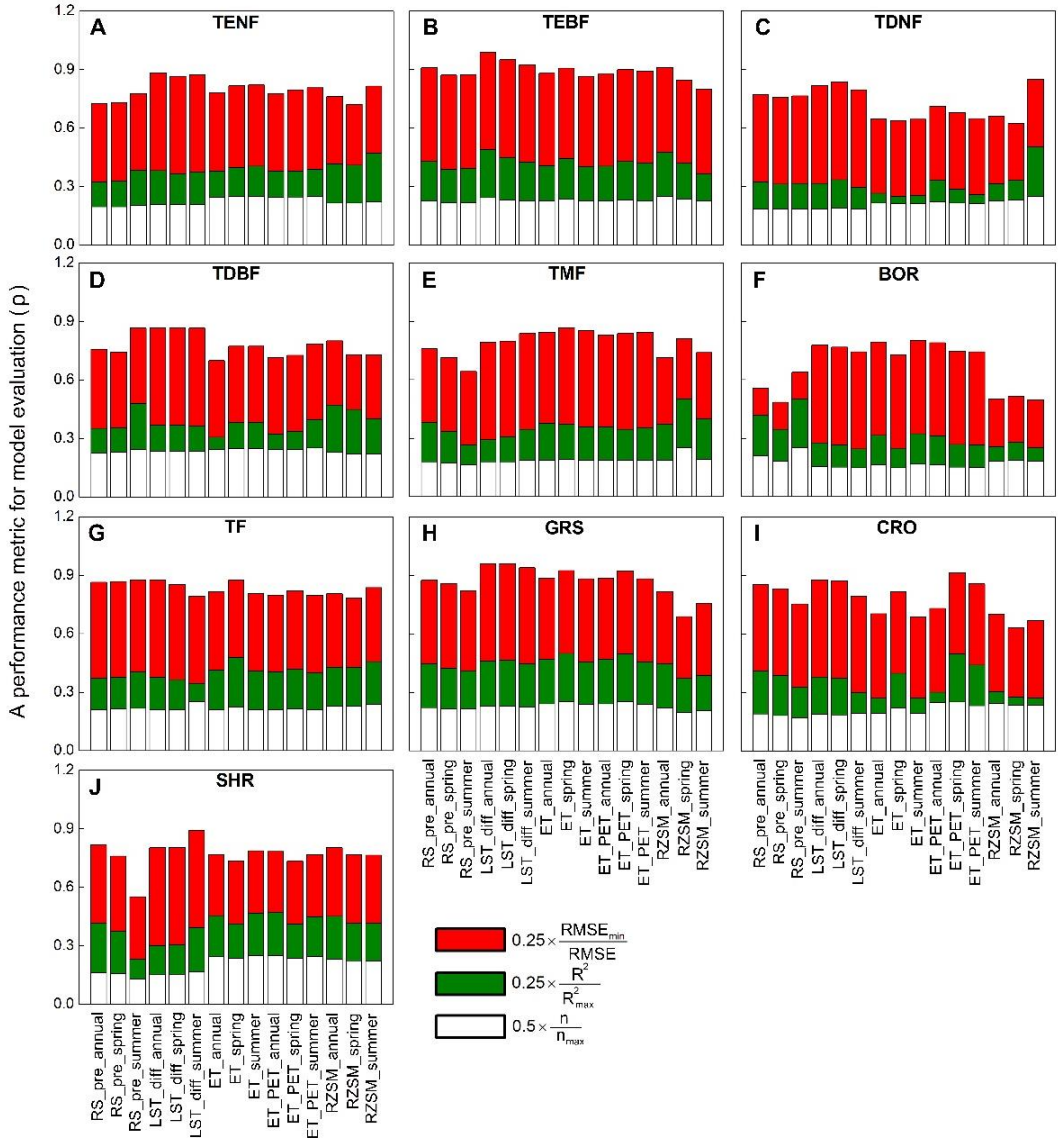

Fig. S12. The performance metric for model evaluation (ρ) for Eq. (3) with different inputs of remotely sensed moisture variables for each biome. Among them, the temperature variable was the selected optimal variable based on the maximum value of ρ in fig. S11. Biome labels are as described in fig. S1.

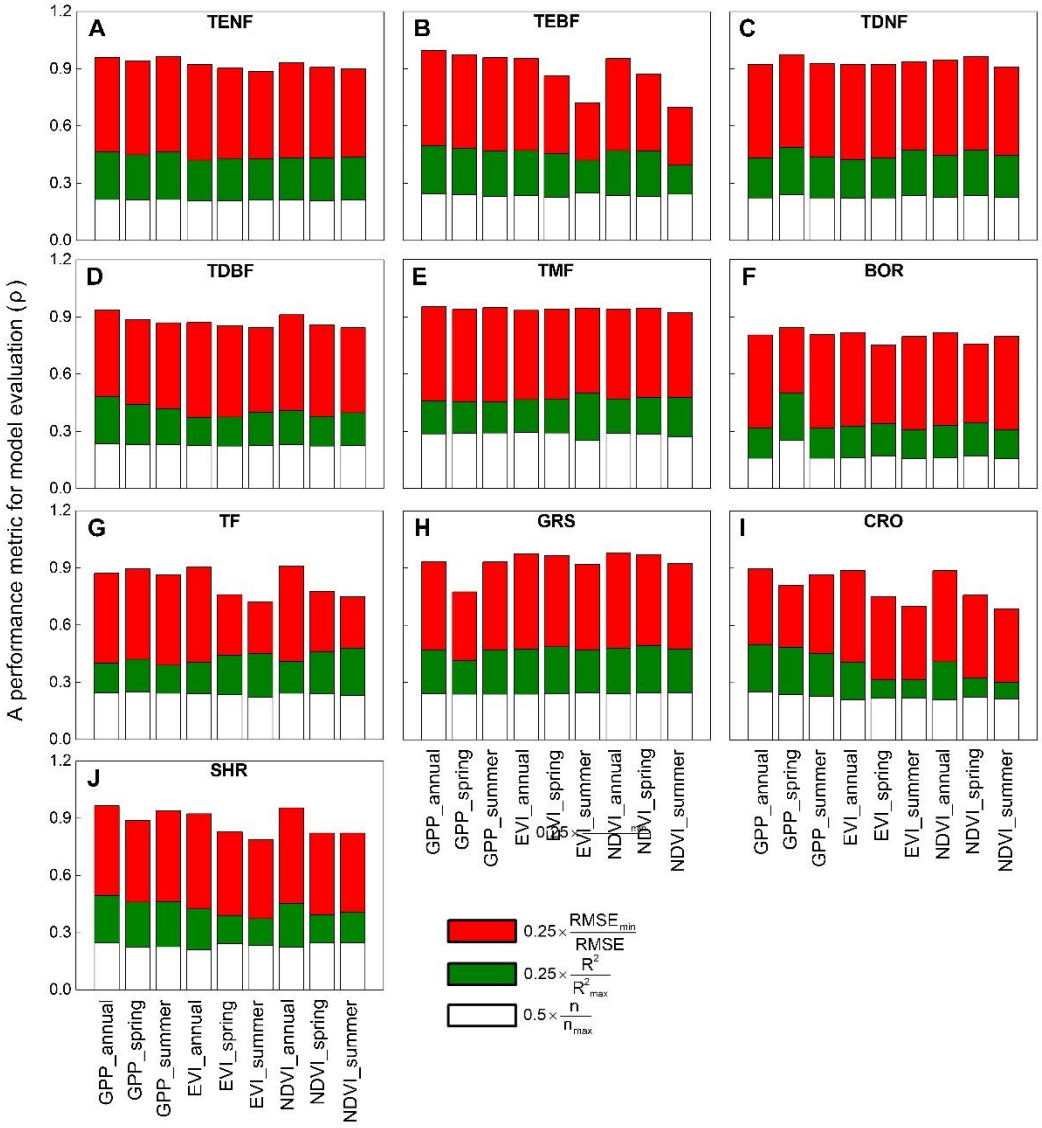

Fig. S13. The performance metric for model evaluation (ρ) for Eq. (4) with different inputs of remotely sensed plant productivity variables for each biome. Among them, temperature and moisture variables were the selected optimal variables based on the maximum of ρ in figs. S11 and S12, respectively. Biome labels are as described in fig. S1.

Table S7. Selected remotely sensed temperature, moisture and plant productivity variables for annual soil respiration (R_s) estimation for each biome.*

Biome	Variables			Eq. 2				Eq.3				MNLR (Eq.4)			
	Temperature	Moisture	Plant productivity	p	n	RMSE	R^2	p	n	RMSE	R^2	p	n	RMSE	R^2
TENF	LST_night_spring	LST_diff_annual	GPP_summer	<0.0001	269	341	0.13	<0.0001	269	332	0.18	<0.0001	264	308	0.30
TEBF	LST_night_summer	LST_diff_annual	GPP_annual	<0.01	53	381	0.17	<0.0001	53	336	0.35	<0.0001	52	293	0.52
TDNF	LST_night_spring	LST_diff_spring	GPP_spring	<0.01	114	306	0.08	<0.0001	114	295	0.15	<0.0001	107	238	0.47
TDBF	LST_night_summer	LST_diff_annual	GPP_annual	<0.0001	230	291	0.09	<0.0001	230	291	0.09	<0.0001	206	274	0.20
TMF	LST_night_annual	ET_spring	GPP_annual	<0.01	66	212	0.15	<0.0001	65	196	0.29	<0.0001	63	186	0.35
BOR	LST_day_annual	ET_summer	NDVI_annual	<0.001	47	170	0.25	<0.0001	45	146	0.45	<0.0001	44	140	0.50
TF	LST_night_spring	LST_diff_annual	NDVI_annual	<0.0001	177	572	0.19	<0.0001	177	555	0.24	<0.0001	166	519	0.36
GRS	LST_night_annual	LST_diff_annual	NDVI_annual	<0.0001	185	494	0.17	<0.0001	185	405	0.45	<0.0001	182	392	0.48
CRO	LST_night_annual	ET_PET_spring	NDVI_annual	<0.0001	83	389	0.25	<0.0001	66	265	0.5	<0.0001	66	254	0.55
SHR	LST_day_summer	LST_diff_summer	NDVI_annual	<0.0001	66	291	0.28	<0.0001	66	259	0.43	<0.0001	64	251	0.45

* Biome labels are as described in fig. S1. RMSE is root mean square error (g C m^{-2} yr^{-1}).

4.1 The selected remotely sensed temperature variables for soil respiration estimation

Regarding the remotely sensed temperature variables, there is no difference among n within each biome (fig. S11). Thus, the selection of the optimal temperature variable for each biome is dependent on the model's explanation capacity. We found that more than half of the selected temperature variables are not at the annual time scale but at the spring and summer time scales (table S7). The selected variable at the spring time scale did not show a significant difference in model explanation capacity than at the annual time scale (one-way ANOVA, $p>0.05$), while a significant difference in model explanation capacity was observed at the summer time scale ($p<0.05$). The reason for this difference may be due to the correlations among these variables. The remotely sensed temperature variables at the spring time scale showed consistently high correlations with the variables at the annual time scale, but the r between the temperature variables at the summer scale and that at the annual time scales were very dynamic. For example, all the r among the remotely sensed temperature variables in the ten biomes were statistically significant ($p<0.001$). However, for the ten biomes, r ranged from 0.91 to 0.97 for the correlation between LST_day_spring and LST_day_annual, from 0.88 to 0.98 for the correlation between LST_night_spring and LST_night_annual, from 0.45 to 0.88 for the correlation between LST_day_summer and LST_day_annual, and from 0.27 to 0.82 for the correlation between LST_night_summer and LST_night_annual (fig. S8). Therefore, we found that the selected LST at the annual or spring time scales for most biomes (table S7) had a similar

ρ (fig. S11) but showed an obvious improvement in ρ over the LST at the summer time scale (relative improvement is greater than 100%, fig. S11).

The selected remotely sensed LST at the summer time scale (i.e., LST_night_summer for TEBF and TDBF, LST_day_summer for SHR) resulted in an obviously higher ρ for Eq. 1 (relative improvement is greater than 15%) than the LST at the annual or spring time scales because of the difference in model explanatory power (i.e., $0.25\times\frac{\mathrm{RMSE}_{\min}}{\mathrm{RMSE}}$ and $0.25\times\frac{\mathrm{R}^2}{\mathrm{R}^2_{\max}}$, fig. S11). For TDBF and TEBF, R_s, associated with obvious plant phonological processes, tends to remain high throughout the summer. Although reduced soil water content decreased the summer R_s in the temperate broadleaf forests when droughts occurred, the temperature still exerted principal control on the annual variation in R_s. Thus, LST_night_summer is the selected optimal temperature variable for R_s estimation in case of TDBF and TEBF (table S7).

Among the selected remotely sensed temperature variables, LST_night was more frequently selected than LST_day (table S7). This result was consistent with previous studies (*18*,*19*) that found that LST_night approximately measured surface air temperature or soil temperature better than LST_day. The reason for this improvement may be due to the light and shadow effects on the LST_day data (*22*). In this study, LST_day_annual was found to be the optimal temperature variable in case of BOR, which may be due to the estimation accuracy of the MODIS LST products. LST_night_annual at the field-measured sites in this biome ranged from -1.2℃ to -15.6°C, while the MODIS LST accuracy was higher than 1°C in the range from −10°C

to 50 ℃. In addition, LST_day explained more R_s spatiotemporal variability than LST_night did for the SHR; and the relationship was robust and not driven by outliers. This may be due to the significant moisture control in SHR because the summer daytime temperature showed a stronger negative correlation with precipitation than nighttime temperature. For example, MAP showed a significantly higher correlation with LST_day_summer ($r=-0.66$, $p<0.0001$) than LST_night_annual ($r=0.36$, $p<0.05$), LST_night_summer ($r=-0.44$, $p<0.01$), and LST_night_spring ($r=0.15$, $p=0.31$).

4.2 The selected remotely sensed moisture variables for soil respiration estimation

In general, n is an important factor for selecting the remotely sensed moisture variables for R_s estimation for each biome (fig. S12). The difference in n for different moisture variables was large for the ten biomes (ratio of the maximum n to the minimum n ranged from 1.2 to 3.7). However, within a single-source moisture variable, the difference in n at the three time scales (i.e., annual, spring, and summer) was negligible, with a maximum coefficient of variance (CV) of less than 10%. For all the forest biomes, RZSM showed a generally higher model explanation capacity than other moisture variables but with a loss of 13% to 37% of the site data (fig. S12) because the root-zone soil moisture product covers the spatial extent of only 60 ℃N-60 ℃S and the time scale of 2002-2010. Thus, the moisture variables calculated from the difference between the MODIS daytime and nighttime LST, with comprehensive temporal and spatial coverages, were selected for annual R_s estimations for most biomes (table S7). In addition, ET-related moisture variables were selected for annual R_s estimations in

case of TMF, BOR and SHR, possibly because ET and ET_PET were better metrics of water availability driving CO_2 exchange in water-limited ecosystems.

4.3 The selected remotely sensed plant productivity variables for soil respiration estimation

Without considering the observation data representation ($0.5\times\frac{n}{n_{max}}$), using GPP, NDVI or EVI at the annual, spring or summer time scales as an input to Eq. 4 led to a similar model explanation capacity for each biome (fig. S13). Thus, the final selection of remotely sensed plant productivity variables for R_s estimation for each biome was greatly dependent on n. Within temperate forest biomes, the difference among n at annual, spring, and summer time scales was small, with a CV less than 1%, and the selected GPP for TENF and TDNF was mainly due to their slightly better model performance (i.e., $0.25\times\frac{RMSE_{min}}{RMSE}$ and $0.25\times\frac{R^2}{R^2_{max}}$) over other variables (fig. S13). However, the difference in n between TF and all the non-forest biomes is relatively large, with a CV lager than 8%, and the n for NDVI or EVI at the annual time scale is greater than for VI at the spring or summer time scale, and GPP at the annual time scale. Thus, NDVI_annual, with the maximum n and a slightly better model explanation capacity, was selected for these biomes (fig. S13). The relatively small n for MODIS GPP in non-forest biomes may be due to the uncertainty in quantifying the water stress factor of MODIS GPP product in water-limited areas, such as SHR and GRS.

Although the role of plant productivity, temperature and moisture interact in eastimating R_s (*56*), we found that remotely sensed plant productivity variables can help

to further explain or more accurately predict R_s variability within biomes (table S7). For instance, in most forest biomes (i.e., TEBF, TDBF, TF) as well as GRS and CRO, remotely sensed plant productivity variables described more of the variation in R_s than the remotely sensed plant productivity variables described in other biomes (fig. S13). The reason for this difference may be a close coupling between the amounts of CO_2 assimilated by forest canopies and released from the soil at an annual time scale.

By gradually adding the selected remotely sensed moisture and plant productivity variables into the model driven by the selected temperature variable for each biome (Eq. 2), the fitting accuracy of Eq. 3 and Eq. 4 greatly improved for most biomes (table S7). For example, compared to Eq. 2, Eq. 3 improved R^2 by more than 82% for TEBF, TDNF, TMF, BOR, GRS, CRO, and SHR. Compared to Eq. 3, Eq. 4 improved R^2 by more than 66% for TENF, TDNF, TDBF, BOR, and SHR. Table S8 describes the results of the multi-collinearity diagnostics for the selected predictive variables used for estimating the annual R_s for the ten biomes. The largest r among the predictive variables used for estimating R_s is 0.78. As variables that qualify for multi-collinearity should have a r value of 0.8 or higher, the problem of multi-collinearity did not exist in our data set.

Table S8. Pearson's correlation coefficient (r) among the remotely sensed temperature, moisture and plant productivity variables for the selected models in ten biomes.*

Biome	Variance	Variance		
		Temperature	Moisture	Plant productivity
TENF	Temperature	1.00	**-0.37**	0.00
	Moisture		1.00	0.07
	Plant productivity			1.00
TEBF	Temperature	1.00	-0.20	**-0.29**
	Moisture		1.00	**0.49**
	Plant productivity			1.00
TDNF	Temperature	1.00	**-0.22**	**-0.32**
	Moisture		1.00	**0.39**
	Plant productivity			1.00
TDBF	Temperature	1.00	**-0.35**	-0.01
	Moisture		1.00	**0.20**
	Plant productivity			1.00
TMF	Temperature	1.00	0.03	**0.45**
	Moisture		1.00	0.21
	Plant productivity			1.00
BOR	Temperature	1.00	**0.52**	0.20
	Moisture		1.00	-0.17
	Plant productivity			1.00
TF	Temperature	1.00	**-0.72**	-0.12
	Moisture		1.00	**0.19**
	Plant productivity			1.00
GRS	Temperature	1.00	**-0.78**	**-0.60**
	Moisture		1.00	**0.59**
	Plant productivity			1.00
CRO	Temperature	1.00	**0.66**	**0.38**
	Moisture		1.00	0.23
	Plant productivity			1.00
SHR	Temperature	1.00	**-0.68**	**-0.52**
	Moisture		1.00	**0.46**
	Plant productivity			1.00

* Biome labels are as described in fig. S1. The values in bold indicate that the Pearson's correlation is statistically significant at $p<0.05$.

5. The model selected to estimate the annual soil respiration for each biome

Among the ten biomes, RFR was the most frequently selected model. It achieved the highest cross-validation accuracy among six biomes (TENF, TEBF, TDBF, TF, GRS, and CRO), and SVR produced the highest cross-validation accuracy for the remaining four biomes. Among these selected machine learning algorithm models, variable importance analysis showed that the remotely sensed temperature variable was the most efficient predictor of R_s in most biomes, followed by the moisture and plant productivity variables (table S9). This finding is consistent with previous studies (*2,10,16*), which suggested that temperature and moisture are the dominant factors regulating global R_s. Furthermore, these selected models exhibited great biases in model predicting accuracy (based on within-sample statistics, table S3) for different biomes. For example, SVR explained more variation in annual R_s for TMF (R^2=0.81, RMSE=119 g C m^{-2} yr^{-1}) and SHR (R^2=0.84, RMSE=153 g C m^{-2} yr^{-1}) than for TDNF (R^2=0.74, RMSE=191 g C m^{-2} yr^{-1}). RFR explained more variation in annual R_s for TENF (R^2=0.71, RMSE=209 g C m^{-2} yr^{-1}) than for TF (R^2=0.63, RMSE=413 g C m^{-2} yr^{-1}).

Table S9. Variable importance analysis of the selected model for each biome.*

Biome	Selected model	Variance importance		
		Temperature	Moisture	Plant productivity
TENF	RFR	1.00	0.93	0.86
TEBF	RFR	0.99	1.00	0.90
TDNF	SVR	1.00	0.83	0.63
TDBF	RFR	1.00	0.99	0.94
TMF	SVR	0.68	1.00	0.63
BOR	SVR	1.00	0.94	0.87
TF	RFR	1.00	0.93	0.91
GRS	RFR	0.93	0.93	1.00
CRO	RFR	0.99	1.00	0.90
SHR	SVR	1.00	0.91	0.61

* Biome labels are as described in fig. S1. RFR is random forest regression and SVR is support vector regression.

Although the model performance with machine learning approaches will greatly improve with gradual increase in number of R_s predictors, the availability of predictor data for application on a large spatial scale and long temporal cover may be greatly reduced (*15*). Considering that highly correlated variables (figs. S8 to S10) did not provide a considerable amount of additional knowledge to the machine learning models, we selected only three variables, which corresponded to the temperature, moisture and plant productivity variables, as inputs to machine learning models. Although previous studies (*3,17*) showed that machine learning models do not greatly suffer from the multi-collinearity problem, reducing the presence of redundant information has proven to be effective in both theory and practice, enhancing the learning efficiency, increasing the predictive accuracy, and reducing the complexity of learned results.

Machine learning algorithms showed higher accuracy in describing R_s spatiotemporal variations than that of MNLR for global biomes based on a ten-fold cross-validation (table S2). MNLR is one of the most frequently used models in R_s estimation because of its simplicity, efficiency, and straightforward interpretation. However, the relationships between R_s and its influencing factors are often complex due to the influences of various biotic and abiotic factors (*56*). Machine learning algorithms do not rely on underlying assumptions about the data and can achieve satisfactory performance through adaptive learning processes, even with a limited number of samples. Compared to MNLR, the high performance of three machine learning models could be due to the existence of a nonlinear relationship between R_s and the predictors that MNLR could not adequately resolve (*17*). Nevertheless, these methods do have some disadvantages, such as the transparency of the resulting models, and the causal relation between the inputs and outputs of the estimation process is not clear, which implies a limited biological interpretation (*2*). This study compensated for this deficiency by performing a variance importance analysis (table S9). Furthermore, the selection process of the input variables based on the fitting accuracy of MNLR also helps to explain the relative role of variables in estimating annual R_s within biomes.

6. The differences between our remote sensing data driven models and previous studies

Our models fundamentally differed from those of previous studies in many ways:

First, most previous studies established statistical regression models for global R_s estimation based entirely on climate data (*9,10,13*). However, we incorporated a plant

productivity factor in the empirical models for each biome, which could provide better estimates of R_s by explaining some of the intersite variability not considered by the climate data driven models. Several authors have noted that considering productivity (for example, GPP) or surrogates of productivity (for example, site-specific leaf area index) improves predictions of annul R_s at the global scale (*9,11*). When R^2 and RMSE were considered, our biome-specific models performed better than previous studies did (table S1). The uncertainty (i.e., 95% CI) calculated by the Monte Carlo method in the present study was less than those in previous studies (table S1). This result did not prove that our method has higher accuracy because the differences existed in the definition and calculation of uncertainty in model parameters between our study and the previous studies. Furthermore, among the ten biomes, the selected optimal model for six biomes is the random forest model (table S2). The reason for the narrow CI may be due to that the performance of the Random forest model usually is not sensitive to the values of numbers of trees and numbers of variables (*17*).

Second, an advantage of the present study was that the estimates are based on the data-driven models that were well constrained by the observed field measurement data and satellite remote sensing data. These data-driven models can provide more data-constrained estimates, but they may not be suitable for long-term estimates because a variety of potential feedback processes should affect R_s flux. Many detailed process-oriented models can provide possible feedback processes but are not easily data-constrained with global datasets, and great uncertainties exist in their estimation (*9*).

Third, our models provide global-scale estimates of annual R_s based on remote sensing variables (temperature, moisture and plant productivity) from 2000 to 2014 with a spatial resolution of 1 km. Our model predictions refer to the mean flux over all the 1 km×1 km grid cells, whereas field measurements are made on the plot, field or stand scales within those grid cells. The scale mismatch between these measured data and gridded remotely sensed variables would inevitably lead to uncertainty in the data available for R_s model establishment.

Fourth, our estimates of R_s can be used independently to estimate the total decomposition in terrestrial ecosystems if a reasonable relationship between R_s and R_h at the annual time scale is defined (similar to the work of Bond-Lamberty and Thomson (*52*)). As spatially and temporally resolved estimates of terrestrial net primary production (NPP) already exist, a combination of our estimates and the previously estimated NPP can be used to gain new insights into terrestrial ecosystem carbon dynamics at the global scale and improve evaluations of the potential impacts of global climate change on terrestrial carbon budgets.